Luminance decay evaluation of the phosphor screen with nanosecond afterglow for low-light-level image intensifier

TIANNING SU[1], FENGGE LIU[1,*], RONGSHENG ZHU[1], BEIHONG LIU[2], SHUAI CHENG[1], MING JI[1], JIE XIAO[1], HANG ZHAO[1], LISONG ZHANG[1], LE CHANG[2], HUIQING YANG[1]
[1]*Department of Operation Support, North Night Vision Technology Co. Ltd., 650217, Kunming, CHN*
[2]*Department of Research and Development, North Night Vision Technology Co. Ltd., 650217, Kunming, CHN*

Luminance decay properties of phosphor screen for low-light-level (LLL) image intensifier is efficiently characterized by the objective measurement of afterglow time. Current measurement precision of afterglow time of phosphor screen for LLL image intensifier reaches only microsecond (μs) level. To achieve the measurement of afterglow time at nanosecond (ns) level, this paper has presented some effective strategies. By establishing luminance decay model of phosphor screen, main factors affecting afterglow time are given. Combining laser diode with signal generator whose sampling frequency of 250 megahertz (MHz), ns light pulse satisfying measurement requirements is generated. Using photomultiplier tube with rising and falling time of 0.57ns, high-speed analog-to –digital converter with sampling frequency of 500MHz, and transimpedance differential amplifier, photocurrent signal at microampere (μA) level has been perfectly processed. At last, through filtering noise accompanying luminance data and acquiring these data based on down sampling, the value of ns afterglow time of phosphor screen can be obtained. Specifically, ns afterglow time of P46 and P47 phosphor screen has been measured. Experimental results show that the average afterglow time of P46 and P47 phosphor screen are 329.79ns and 118.09ns, respectively. Both repetitive errors are 0.013 and 0.021, respectively. These measured data clearly demonstrate that effective evaluation of luminance decay of phosphor screen with ns afterglow time for LLL image intensifier can provide a strong tool for reasonable selection of high quality phosphor used in night vision devices.

(Received August 28, 2023; accepted February 12, 2024)

Keywords: Luminance decay, nanosecond afterglow, phosphor screen, Low-light-level image intensifier

1. Introduction

Ultrafast low-light-level (LLL) image intensifiers have been used in a wide range of applications including transient frame imaging, biomedicine, high energy physics and scientific research [1-4]. One of the most important components of these image intensifiers is an ultrafast -response phosphor screen with nanosecond (ns) afterglow time, which can be obtained by two types of phosphors such as P46 and P47 [5-7]. Consequently, more attention needs to be focused on evaluation of luminance decay properties of this ultrafast-response phosphor screen [8]. In particular, a precise measurement of afterglow time of phosphor screen is essential. Naturally, some meaningful work has been reported so far [9-14]. In these work, the excitation sources for afterglow time measurement mainly include light pulse and gated photocathode voltage pulse. The light pulse can be easily obtained by controlling electromechanical shutter, however, the descent velocity and the duration of this light pulse could satisfy only millisecond afterglow time measurement. Additionally, the measurement limitation of gated photocathode voltage pulse is microsecond, which is insufficient to measure nanosecond afterglow time [15].

In order to achieve the goal of nanosecond afterglow measurement of phosphor screen for LLL image intensifier, we will introduce some effective strategies. By establishing the luminance decay model of phosphor screen, main factors affecting the afterglow time will be given, and then the decay evaluation criteria will be determined. Sequentially, the excitation source is light pulse generated by combining laser diode with function generator whose sampling frequency is 250 megahertz(MHz). The selection of photomultiplier tube (PMT) with rise time and fall time of 0.57ns is sufficient to measure the afterglow time. Through high-speed analog-to-digital converter (ADC) chip with sampling frequency of 500MHz and transimpedance differential amplifier, photocurrent signal at microamp (μA) level will be perfectly processed. At last, by filtering noise from luminance data of phosphor screen and acquiring these data based on down sampling, the nanosecond afterglow time can be obtained. As a result, luminance decay evaluation of the phosphor screen with nanosecond afterglow for LLL image intensifier will be implemented.

2. Strategies to measure ns afterglow time

2.1. Establishing luminance decay model

The basic function of the phosphor screen is to convert the electron beam to light. Light emission occurs when the excited states return to their normal state. Fig.1 shows the energy band diagram of a phosphor in a general state.

Luminescence is related with the presence of localized energy levels in normally forbidden gap.

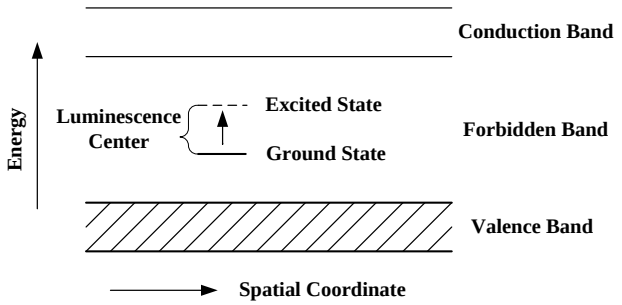

Fig. 1. Energy band schematic diagram of a phosphor

In absence of excitation, when time in seconds t=0, the number $n(t)$ of electrons in ground state at random time varies with changing t. Assuming that τ is average lifetime of carriers in excited state, and $dn(t)/dt$ denotes the number of reduced carriers in excited state per second, the number of photons transiting from these carriers per second is defined as

$$-\frac{dn(t)}{dt}=\frac{n(t)}{\tau} \tag{1}$$

By integration equation (1), the following equation is obtained

$$n(t)=n_0e^{-\frac{t}{\tau}} \tag{2}$$

where n_0 is the number of carriers in excited state before light source is removed. If photons are released when electrons transit from excited state to ground state, the luminescence intensity is in direct proportion to the number of electrons in excited state, namely, this expression is given by

$$I(t)=Kn(t)=Kn_0e^{-\frac{t}{\tau}}=I_0e^{-\frac{t}{\tau}} \tag{3}$$

where K is proportionality coefficient, and I_0 represents maximum value of luminescence intensity before light source is removed. From equation (3), it is clear that luminance decay appears in exponential law. It should be emphasized that afterglow time is defined as time interval which the luminance intensity falls from I_0 to 10% of I_0.

As is well known, the generation rate of electron-hole pairs of luminescence center in equilibrium state is equal to the recombination rate of them, namely, the number of electrons keep constant. Therefore, the stability condition is defined by

$$r_nn(N_t-n_t)+r_pp_1(N_t-n_t)=r_nn_1n_t+r_ppn_t \tag{4}$$

where r_n is electron capture coefficient, r_p is hole capture coefficient, n is electron concentration in conduction band, p is hole concentration in valence band, n_t is electron concentration at luminescence center level, N_t is concentration in luminescence center, p_1 denotes hole concentration in valence band when Fermi level overlaps with luminescence center level, n_1 represents electron concentration in conduction band when Fermi level overlaps with luminescence center level, respectively.

From equation (4), we can obtain the recombination rate of noequilibrium carriers L as follows:

$$L=\frac{N_tr_pr_n(np-n_t^2)}{r_n(n+n_1)+r_p(p+p_1)} \tag{5}$$

Obviously, since $np=n_t^2$ under thermal equilibrium condition, L is zero. Whereas, when the conditions of semiconductor material are changed, such as increasing incident light intensity and raising temperature, noequilibrium carriers would be injected into semiconductor material. Correspondingly, substituting $n=n_0+\Delta n$, $p=p_0+\Delta p$, and $\Delta n=\Delta p$ into equation (5), the expression of L is of the form

$$L=\frac{N_tr_pr_n(n_0\Delta p+p_0\Delta p+\Delta p^2)}{r_n(n_0+n_1+\Delta p)+r_p(p_0+p_1+\Delta p)} \tag{6}$$

Besides, the average lifetime of carriers in excited state is given by

$$\tau=\frac{\Delta p}{L}=\frac{r_n(n_0+n_1+\Delta p)+r_p(p_0+p_1+\Delta p)}{N_tr_pr_n(n_0+p_0+\Delta p)} \tag{7}$$

As can be seen from equation (7), the average lifetime τ of carriers in excited state is inversely proportionally to the concentration N_t of luminescence center, i.e., τ decreases with increasing N_t.

According to the luminance formula of phosphor screen for LLL image intensifier [15], the phosphor screen current I_p is given by

$$I_p=D_{cv}ES_cA_cG_m \tag{8}$$

where D_{cv} is the duty circle of photocathode voltage pulse, E is photocathode illumination, S_c is photocathode sensitivity, A_c is the incident light area of photocathode, and G_m is current gain of microchannel plate (MCP), respectively. Considering that the changes in phosphor screen current lead to the changes in conductivity, the modified formula of changes $\Delta\sigma$ in noequilibrium carriers is defined by

$$\Delta\sigma=\Delta nq\mu_n+\Delta pq\mu_p=\Delta pq(\mu_n+\mu_p) \tag{9}$$

where q is electron charge, μ_n is electron mobility, and μ_p is hole mobility.

In conclusion, luminance decay model of phosphor screen for LLL image intensifier can be established as follows

$$\begin{cases} I(t) = I_0 e^{-\frac{t}{\tau}} \\ \tau = \dfrac{r_n(n_0 + n_1 + \Delta p) + r_p(p_0 + p_1 + \Delta p)}{N_t r_p r_n (n_0 + p_0 + \Delta p)} \\ N_t = \alpha \Delta p = \alpha \dfrac{\Delta I_p l}{V_p s q(\mu_n + \mu_p)} (\alpha > 0) \\ \Delta I_p = D_{cv} S_c A_c G_m \Delta E \end{cases} \quad (10)$$

where α denotes the rate of change in concentration of carriers in luminescence center per second, V_p is phosphor screen voltage, s is sectional area of phosphor screen, l is equivalent length of semiconductor material. From equation (10), it is clear that, as incident illumination is increased or temperature is raised, the concentration of carriers in luminescence center is increased because the number of noequilibrium carriers participating in transition becomes large. In consequence, the afterglow time of phosphor screen is reduced along with decreasing the lifetime of those carriers. From a practical standpoint, by varying incident electron current density, corresponding values of afterglow time of P46 and P47 phosphor screens for LLL image intensifier can be measured.

2.2. Generating ns light pulse

As a necessary component of measurement system of afterglow time, the performance of light source is crucial. In a bid to obtain ns light pulse, we have employed laser diode driven by high-speed function generator as the excitation source. To be more specific, we have selected type of Osram PLT5-510 laser diode whose output power is 10milliwatt (mW) and drive current is in the range of 45~75 milliampere (mA). Meanwhile, the type of Tektronix AFG31251 function generator with sampling frequency of 250 MHz is used, since it can generate square-wave pulse with minimum period of 4ns. Moreover, the duty circle of this generator is easily adjusted, and the rise edge and fall edge of square-wave pulse can be reduced to 2ns. Through changing values of output voltage of function signal generator, the drive current of laser diode can be conveniently regulated. Based on a combination of laser diode and function signal generator operated in continuous mode, ns light pulse satisfying the measurement requirement can be successfully obtained.

2.3. Capturing luminance signal

The measurement of ns afterglow time of phosphor screen for LLL image intensifier must be carried out in a black box. In this black box, there are a collimator with inner diameter of 25millimeter (mm), a PMT, a text fixture of inner diameter of 25mm, and auxiliary transmission interface. According to the frequency of square-wave pulse, the excited source alternates in between light and dark. In sequence, this light is converted into uniform light within the integrating sphere, and the diffused uniform light enters LLL image intensifier along with collimator, photoelectrons are multiplied by MCP and will bombard phosphor screen. Ultimately, the luminance signal of phosphor screen occurs.

The selection of PMT (Hamamatsu H10721) with rise time and fall time of 0.57ns can meet measurement requirements of ns afterglow time of phosphor screen. Since the output photocurrent of PMT is in μA, it is necessary to design transimpedance differential amplifier so that this photocurrent signal in μA can be converted to manageable voltage signal. To capture luminance signal, we have employed AD9684 chip which has time resolution of 2ns and 14-bit resolution. Additionally, the clock pulse of 1Gigahertz (GHz) is generated by ABLIC AX5 crystal oscillator, which can satisfy the requirement owing to clock skew of 115femtosecond (fs). The 14-channel differential signal generated by AD9684 and the clock signal enter into field programmable gate array (FPGA) via FPGA Mezzanine Card. So far, the luminance signal can be captured.

2.4. Filtering and fitting luminance data

In order to avoid delay error caused by filter capacitor, any filter capacitor has not been included in transimpedance differential amplifier. Unfortunately, the granularity noise of phosphor screen is introduced into luminance signal, which leads to imprecise afterglow time of phosphor screen will be obtained. Hence, it is important to filter luminance data.

Here, precise luminance data can be obtained by Kalman Filter, and the determination of Kalman gain coefficient K_g is the most important. In our work, after many experiments, K_g is given by

$$K_g = \frac{Q_n}{Q_n + R_n} \quad (11)$$

where Q_n signifies covariance matrix of system noise, R_n denotes covariance matrix of observation noise, respectively. Concretely, the value of K_g is closer to 1 indicates that optimum estimation value is closer to theoretical value, whereas the value of K_g is closer to zero shows that optimum estimation value is closer to observation value. During the measurement of afterglow time of phosphor screen for LLL image intensifier, the value of Q_n is 0.001, and the value of R_n is 0.5.

To acquire precise positioning of falling edge of luminance signal of phosphor screen, fitting those filtered luminance sampling data and using exponential damping polynomial as model must be done. By adopting the method of quick search falling edge based on down sampling, the starting point of afterglow is roughly determined when continuous 5 sample data appear monotonically decreasing per 20 sample data. By extracting 1000 sample data before this starting point and 500 sample data after the same

starting point, these 1500 sample data are fitted for processing. Note that this start point of afterglow is roughly given, for the sake of obtaining precise position of start point, it is necessary to determine a standard value of high level from the average value of 1000 sample data. The precise start point of afterglow measurement should be defined as corresponding abscissa of the first value larger than this standard value of high level. So, luminance data fitting can be divided into two parts: (a) sampling data at high level uses polynomial fitting method; (b) sampling data of afterglow process uses exponential damping polynomial fitting method. Fig.2 shows fitted curve of luminance sampling. Because the sampling accuracy of AD chip is 14-bit and transmits differential signals, corresponding amplitude range of digital signals is from -8192 to 8192 which is illustrated in vertical axis. According to this curve in Fig.2, we can calculate the afterglow time and further complete luminance decay evaluation of ns afterglow time of phosphor screen for LLL image intensifier.

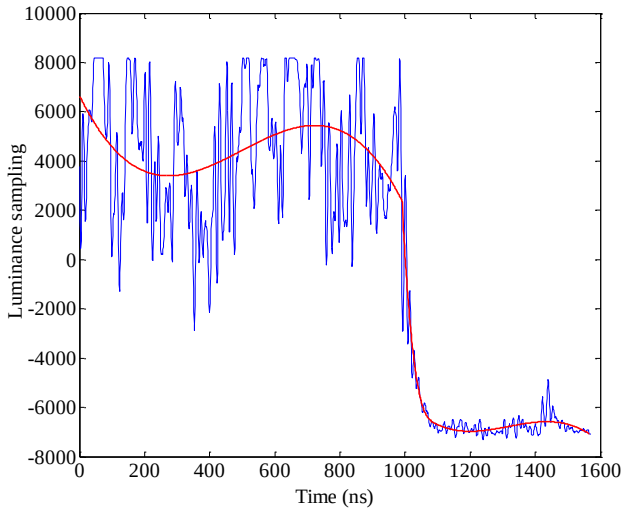

Fig. 2. Fitted curve of luminance sampling (color online)

2.5. Evaluating luminance decay properties

Luminance decay evaluation of phosphor screen with for LLL image intensifier is strongly demonstrated by measuring its afterglow time. Figs.3a and 3b show the measurement system of ns afterglow time for LLL image intensifier. The operating principle of this measurement system is as follows: light pulse satisfying the measurement requirements is generated by laser diode driven by high-speed signal generator; this light pulse enters into black box where LLL image intensifier is placed via integrating sphere; weak luminance signal is detected by PMT and is converted into photocurrent in μA; this photocurrent signal can be effectively amplified and processed so as to be filtered and to fitted; finally, the nanosecond afterglow time of phosphor screen for LLL image intensifier can be obtained.

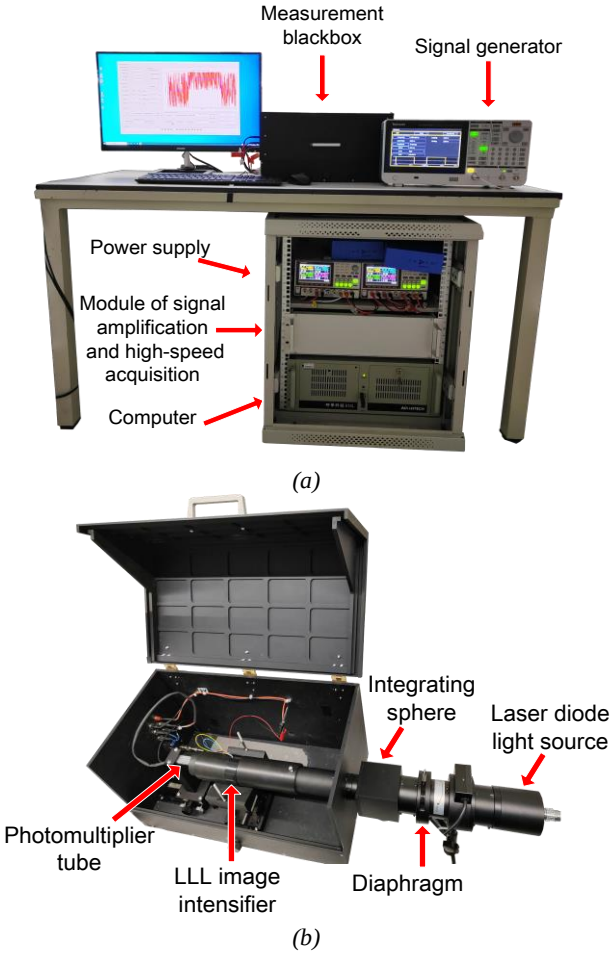

Fig. 3. (a) Picture of measurement system of ns afterglow time of phosphor screen for LLL image intensifier; (b) Picture of inside structure and outside connection of measurement black box (color online)

Moreover, it is important to notice that the afterglow time of P46 and P47 phosphor screen need to be measured ten times, the average value of these 10 measured results is defined by the afterglow time. Here, the relative error of measured results is characterized by repetitive error ε. The expression of ε is given by

$$\varepsilon = \frac{\sqrt{\sum_{i=1}^{n}(x_i - \bar{x})^2 \Big/ (m-1)}}{\bar{x}} \tag{12}$$

where x_i is the measured value of each time, $\bar{x}$ is average value of 10 measured results, m is measurement times, here, the value of m is 10. So definitely, a smaller repetitive error ε demonstrates that this measured result is more accurate.

3. Results and discussions

3.1. Setting measurement conditions

Prior to measurement of nanosecond afterglow time of P46 and P47 phosphor screens for LLL image intensifiers, high level voltage of Tektronix AFG31251 signal generator must be calibrated by optical power meter according to general specification of GJB 7351-2011. More specifically, the value of high level voltage driving laser diode from this signal generator is adjusted between 1.75V and 1.85V. The parameters of square-wave pulse used in measurement of afterglow time P46 and P47 phosphor screens are shown in Table 1.

Table 1. Parameters of square-wave pulse

Parameter	Value
Frequency (KHz)	100
Amplitude (V)	1.75~1.85
Duty circle (%)	50~90
Rising time (ns)	2
Falling time (ns)	2

3.2. Measured result of delay time of system

In order to avoid the effect of inherent delay time of system on afterglow time of phosphor screen, delay time of excited source, PMT, and circuit of high-speed signal processing must be measured in the first place. In other words, luminance signal from black box without LLL image intensifier need to be acquired. Therefore, when the duty circle of square-wave pulse is 60%, high-level voltage is 2.20V, and gain voltage of PMT is 0.90V, continuous measured results of ten times pertaining to delay time of falling edge are shown in Table 2.

Table 2. Delay time of falling edge of measurement system

Order	Delay time (ns)	Average delay time (ns)	Repetitive error
1	12.64		
2	11.82		
3	12.46		
4	10.85		
5	11.06	11.66	0.053
6	11.53		
7	11.48		
8	12.20		
9	10.98		
10	11.54		

As can be seen from Table 2, the average delay time of measurement system is about 11.66ns, and the repetitive error is about 0.053. Note that the delay time of 11.66ns has a little impact on measured result of ns afterglow time of phosphor screen for LLL image intensifier. There is still room for further reduction in the delay time.

3.3. Measured result of afterglow time of P46

Specific measurement conditions of afterglow time of P46 phosphor screen are given that the duty circle of excited pulse is 60%, high-level voltage is 1.75V, and gain voltage of PMT is 0.70V, respectively. Under these conditions, the afterglow time of P46 phosphor screen is measured consecutively ten times. Table 3 shows ten measured results, the average value of ten results, and repetitive error.

Table 3. Measured afterglow time of P46 phosphor screens

Order	afterglow time (ns)	Average afterglow time (ns)	Repetitive error
1	324.22		
2	330.43		
3	332.44		
4	334.11		
5	328.28	329.79	0.013
6	325.65		
7	328.42		
8	331.31		
9	325.58		
10	337.53		

Selecting a falling edge of luminance curve of P46 phosphor screen at random, corresponding luminance delay characteristics and afterglow time are illustrated in Fig. 4 (a-d).

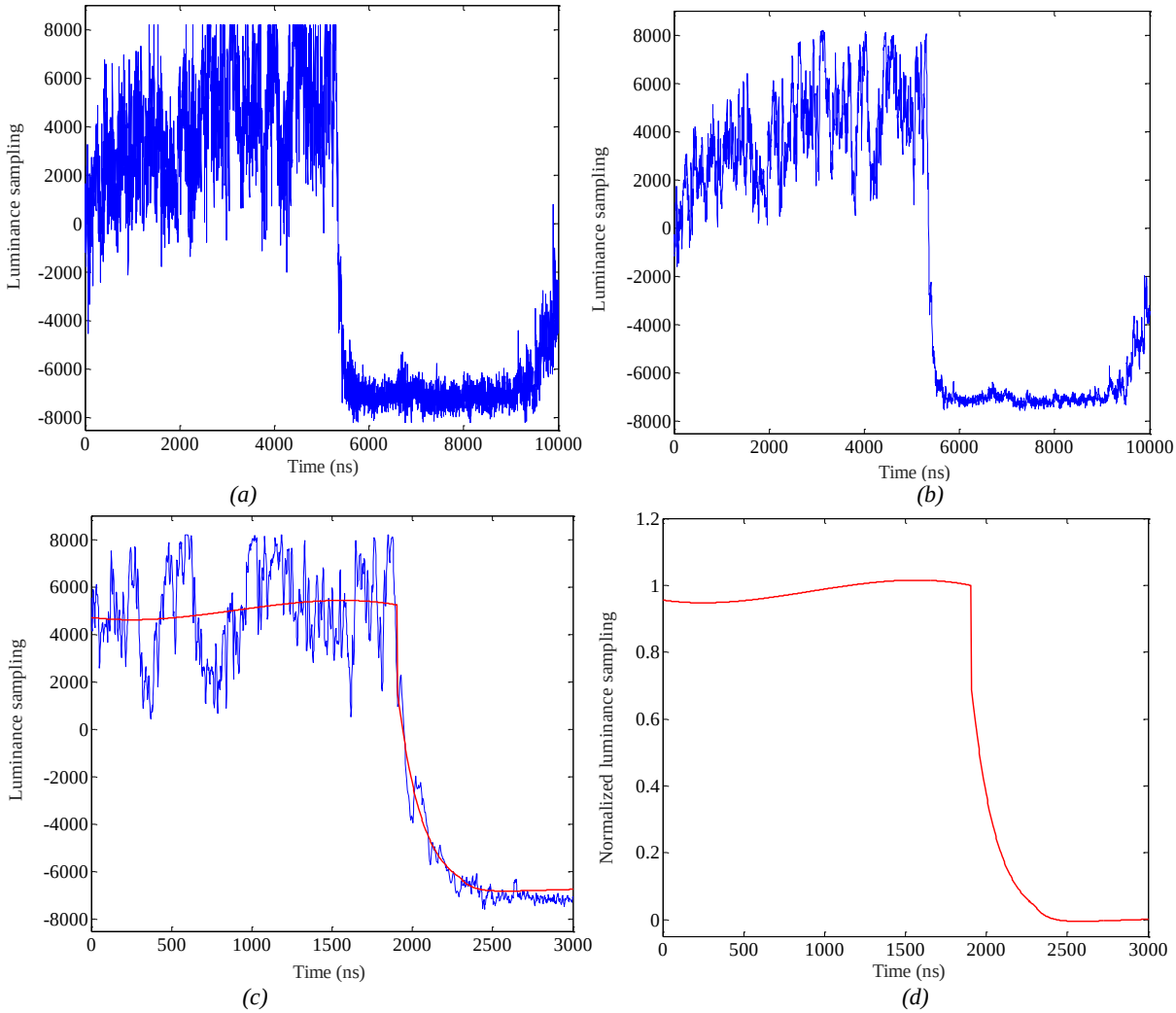

Fig .4. (a) Initial luminance curve of any falling edge of P46 phosphor screen; (b) Filtered luminance curve of any falling edge of P46 phosphor screen; (c) Fitted luminance curve of any falling edge of P46 phosphor screen; (d) Normalized luminance curve of any falling edge of P46 phosphor screen (color online)

The typical value of afterglow time of P46 phosphor screen is about 300ns [16]. From the data of Table 3 and Figs.4a-4d, it is clear that the average measured value of afterglow time of P46 phosphor screen is 329.79ns, and repetitive error is only 0.013. Considering the intrinsic delay time of 11.66ns, this measured result is satisfactory and the measurement system is capable of evaluating luminance decay properties of phosphor screen with ns afterglow time for LLL image intensifier.

3.4. Measured result of afterglow time of P47

To further verify the reliability and flexibility of the above measurement system, on the same conditions as P46 phosphor screen, the afterglow time of P47 phosphor screen is measured ten times, and corresponding measured results and repetitive error are shown in Table 4.

Table 4. Measured afterglow time of P47 phosphor screens

Order	afterglow time (ns)	Average afterglow time (ns)	Repetitive error
1	118.49	118.09	0.021
2	118.21		
3	113.36		
4	122.08		
5	120.73		
6	116.25		
7	117.44		
8	117.58		
9	119.99		
10	116.80		

Selecting a falling edge signal of afterglow curve of P47 phosphor screen at random, corresponding luminance delay characteristics and afterglow time are shown in Figs.5a-5d.

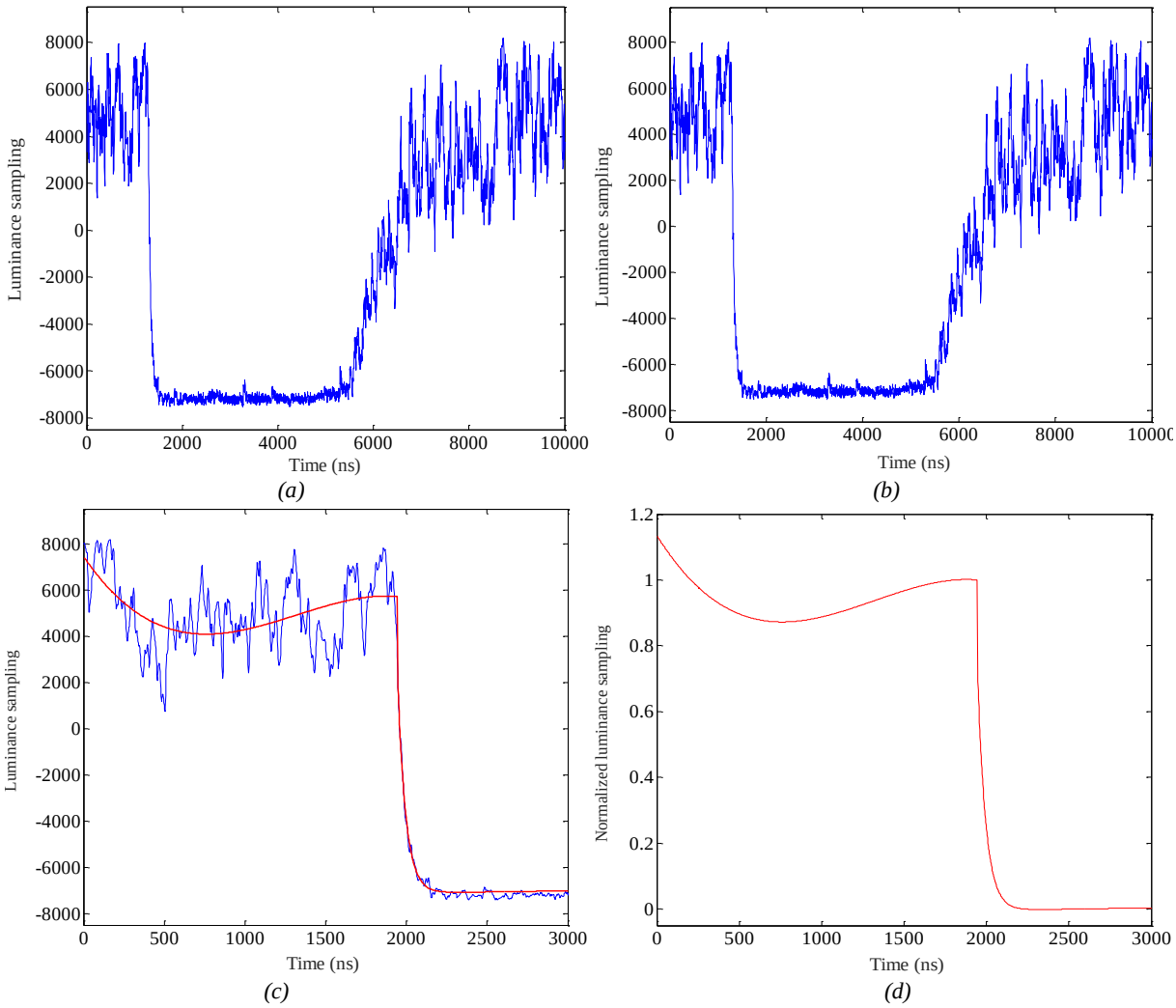

Fig. 5. (a) Initial luminance curve of any falling edge of P47 phosphor screen; b. Filtered luminance curve of any falling edge of P47 phosphor screen; c. Fitted luminance curve of any falling edge of P47 phosphor screen; d. Normalized luminance curve of any falling edge of P47 phosphor screen (color online)

The typical value of afterglow time of P47 phosphor screen is approximately 100ns [16]. Table 4 and Figs.5a-5d show that measured afterglow time ranges from approximately 113ns to 122ns, the average afterglow time is about 118.09ns, and repetitive error is 0.021, respectively. If the intrinsic delay time of 11.66ns generated from the measurement system is eliminated, the data of Table 4 has proven its objectivity and reliability. Combining measured results of afterglow time of P46 and P47 phosphor screen, it can be said that this measurement system must be able to effectively evaluate luminance decay properties of phosphor screen with ns afterglow time for LLL image intensifier.

3.5. Effect of electron current density on afterglow time of P46 and P47

The model of luminance decay of phosphor screen has played a crucial role in the measurement of afterglow time.

Based on this model and corresponding calculation, main factors affecting the afterglow time have been given and appropriate measurement conditions have been determined.

According to this model, we can conclude that the afterglow time decreases with increasing the density of incident electron current. In a bid to verify the validity of the luminance decay model, it is necessary to make clear the effect of electron current density on the afterglow time of P46 and P47 phosphor screen. Hence, by adjusting high-level voltage of signal generator and then varying driving current of laser diode, the density of incident electron current can be changed. Naturally, the dependence of the luminance decay of phosphor screen on electron current density is demonstrated by measuring the afterglow time at different voltages. Table 5 shows the measured value of afterglow time of P46 and P47 phosphor screen at different high-level voltages.

Table 5. Measured afterglow time at different voltages

Phosphor Screen	High-level voltage (V)	Afterglow time (ns)
P46	1.85	328.69
	1.82	330.61
	1.78	334.36
	1.75	337.53
P47	1.85	116.85
	1.82	117.63
	1.78	119.84
	1.75	121.36

The most striking feature in Table 5 is the reduced afterglow time as high-level voltage increases. It is mainly explained by the fact that the number of incident photon arriving at photocathode surface becomes larger as electron current density increases, that is to say, the probability of electrons transited from filled band to conduction band increases. Since electrons captured by trap may form recombination luminescence, the lifetime of carriers in conduction band is reduced, and then the aftertime time is shortened. As a consequence, the validity of luminance decay model has been verified.

4. Conclusions

The effective measurement of afterglow time of phosphor screen is a strong tool for the evaluation of luminance decay of phosphor screen. Currently, the measurement precision limitation of afterglow time of phosphor screen for LLL image intensifier can only reach μs level, which is insufficient to measure ns afterglow time of phosphor screen for LLL image intensifier. To achieve this goal, some effective strategies have been introduced. These strategies mainly include the determination of main factors affecting afterglow time, the generation of ns light pulse, the capture and amplification of photocurrent at μA level, filtering of noise accompanying luminance signal, and fitting process of luminance sampling data.

By solving above difficulties, a measurement system of ns afterglow time of phosphor screen for LLL image intensifier has been designed. More importantly, the ns afterglow time of P46 and P47 phosphor screen has been successfully measured. Experimental results show that the average afterglow time of P46 and P47 are 329.79ns and 118.09ns, respectively. Additionally, both repetitive errors are 0.013 and 0.021, respectively. Considering the intrinsic delay time of 11.66ns from measurement system, these measured data clearly demonstrate that our strategies to evaluate luminance delay properties of phosphor screen by means of measuring ns afterglow time are very effective. In practice, effective evaluation of luminance decay of ns afterglow time of phosphor screen for LLL image intensifier can provide a powerful tool for the reasonable selection of high quality phosphor used in night vision devices. To improve measurement accuracy, it is of considerable interest to further reduce the intrinsic delay time of measurement system to below 11.66ns.

Acknowledgements

All authors thank Zhiyun Pan for his useful discussions.

References

[1] T. Q. Gao, G. D'Amen, S. Burdin, M. Alsulimane, P. Campbell, C. D. Via, A. Nomerotski, A. Roberts, P. Svihra, K. Mavrokoridis, J. Taylor, A. Tricoli, Nucl. Instrum. Methods Phys. Res. Sect. A **1046**, 167604 (2023).
[2] R. Sen, A. V. Zhdanov, C. Devoy, M. Tangney, L. M. Hirvonen, A. Nomerotski, D. B. Papkovsky, J. Vis. Exp. **194**, e64321 (2023).
[3] Q. Shen, J. S. Tian, C. Q. Pei, Sensors **22**(19), 7372 (2022).
[4] H. Sparks, F. GÖrlitz, D. J. Kelly, S. C. Warren, P. A. Kellet, E. Garcia, A. K. L. Dymoke-Bradshaw, J. D. Hares, M. A. A. Neil, C. Dunsby, P. M. W. French, Rev. Sci. Instrum. **88**, 013707 (2017).
[5] K. A. Vereschagin, N. S. Vorobev, P. B. Gornostaev, E. I. Zinin, S. R. Ivanova, T. P. Kulichenkova, G. P. Levina, V. I. Lozovoi, V. A. Makushina, O. I. Meshkov, Y. M. Mikhalkov, Z. M. Semichastnova, A. V. Smirnov, E. V. Shashkov, M. Y. Schelev, J. Russ. Laser Res. **35**(6), 617 (2014).
[6] Y. Suda, Y. Tamura, S. Yamaguchi, Y. Nanai, T. Okuno, J. Phys. D: Appl. Phys. **54**(41), 415103 (2021).
[7] M. Fisher-Levine, A. Nomerotskl, J. Instrum. **11**, C03016 (2016).
[8] T. Jiang, H. Wang, M. M. Xing, Y. Fu, Y. Peng, X. X. Luo, Physica B **450**, 94 (2014).
[9] P. Scajev, A. Mekys, J. Instrum. **18**(5), P05026 (2023).
[10] Y. M. Fang, Y. S. Gou, M. R. Zhang, J. F. Wang, J. S. Tian, Nucl. Instrum. Methods Phys. Res. Sect. A **987**, 164799 (2021).
[11] V. V. Postupaev, Nucl. Instrum. Methods Phys. Res. Sect. A **923**, 147 (2019).
[12] M. Zhang, L. Sheng, H. S. Hu, Y. Li, Y. T. Liu, D. W. Hei, B. D. Peng, J. Z. Zhao, IEEE T. Nucl. Sci. **65**(8), 2310 (2018).
[13] Y. X. Chen, S. L. Zhao, Z. Xu, C. W. Zhang, X. R. Xu, Spectrosc. Spect. Anal. **37**(7), 1993(2017).
[14] Z. Mazurak, A. Wanic, J. Karolczak, M. Czaja, J. Lumin. **158**, 103(2015).
[15] M. H. Sun, Y. S. Qian, Y. N. Ren, Q. Zhi, X. Y. Kong, Y. Z. Lang, Acta Photonica Sinica **51**(3), 0304004 (2022).
[16] I. P. Csorba, Image Tubes, Howard W. Sams & Co., Inc., Indianapolis, 1986.

*Corresponding author: lfg15925147665@163.com